METEOROLOGICAL APPLICATIONS
Meteorol. Appl. **14**: 403–412 (2007)
Published online in Wiley InterScience
(www.interscience.wiley.com) DOI: 10.1002/met.39

RMetS
ROYAL METEOROLOGICAL SOCIETY

Sensing of diurnal and semi-diurnal variability in the water vapour content in the tropics using GPS measurements

Surat Pramualsakdikul,* Rüdiger Haas,* Gunnar Elgered and Hans-Georg Scherneck
Department of Radio and Space Science, Chalmers University of Technology, Onsala Space Observatory, SE- 439 92 Onsala, Sweden

ABSTRACT: The diurnal and semi-diurnal variability of the integrated precipitable water vapour (IPWV) was studied by using Global Positioning System (GPS) data (1998–2004) from 14 International GNSS Service (IGS) stations located between latitudes 20 °S and 20 °N, and longitudes 70°–170 °E. The phases and amplitudes of the IPWV are compared to the corresponding estimates from two numerical weather models (NWMs). Results reveal that there are diurnal amplitudes of more than 0.4 mm for most sites, except sites on small islands in the ocean. The maximum diurnal amplitude is 3 mm at Bakosurtanal, Indonesia. The estimated semi-diurnal signals are in general small. The maximum of the IPWV typically occurs between 1200 and 2400 local solar time. The results suggest that GPS data are useful for high-temporal-resolution studies of IPWV. The accuracy of the estimated diurnal amplitudes is limited by the use of a simple model for the mean temperature of the wet refractivity, and the accuracy of the estimated semi-diurnal amplitudes is likely to be improved by a higher temporal resolution of the ground pressure data at the GPS sites. Copyright © 2007 Royal Meteorological Society

KEY WORDS water vapour; GPS; diurnal; semi-diurnal; tropical atmosphere

Received 21 February 2007; Revised 30 July 2007; Accepted 26 September 2007

1. Introduction

Water vapour is the most abundant and important greenhouse gas. It is also one of the most variable atmospheric parameters both in time and space. It has a central influence on atmospheric radiation and the hydrological cycle. Therefore, the daily variation in the integrated precipitable water vapour (IPWV) in the atmosphere is an interesting topic for many studies (Güldner and Spänkuch, 1999; Bouma and Stoew, 2001; Dai *et al*., 2002).

Many techniques are used to study atmospheric water vapour. Radiosondes are a common tool used to record meteorological profiles, i.e. temperature, humidity, wind (speed and direction) and air pressure in the vertical direction. They can operate up to 30 km from the ground. Owing to the high cost for each launch, they are typically launched only twice daily. Launches are often performed at specific sites (e.g. airports and meteorological offices). With an uneven spatial coverage and poor temporal resolution, the radiosonde technique is not ideal for monitoring of fairly rapid variation of IPWV in the atmosphere.

Ground-based, upward-looking microwave radiometers can be used to measure water vapour directly with a time resolution of seconds, and the accuracy can be better than that of conventional radiosondes. Ground-based microwave radiometry has the advantage of near all-weather capability but the technique does not work in the case of precipitating clouds (Güldner and Spänkuch, 1999). Furthermore, it gives poor spatial resolution since only a few instruments are operational in a continuous mode. The specific application of estimating weak diurnal signals in the IPWV is difficult because of expected temperature-dependent systematic measurement errors. Several instruments and sensors on satellites can also be used to measure atmospheric water vapour, e.g. the Advanced Microwave Sounding Unit (AMSU-B). These techniques provide good spatial but poor temporal resolution (Vey *et al*., 2004).

It has been shown that it is possible to study diurnal and semi-diurnal variations of IPWV using ground-based Global Positioning System (GPS) data. Dai *et al*. (2002) studied the diurnal (S_1) and semi-diurnal (S_2) variability using GPS data from 54 North American sites spanning the period 1996–2000. The amplitudes of the diurnal cycle were found to be 1.0–1.8 mm and the peaks occurred around noon in winter and between mid-afternoon and midnight in summer, whereas the semi-diurnal amplitudes were weak, on the order of some tenths of a millimetre. Güldner and Spänkuch (1999) found a weak diurnal cycle in the IPWV from ground-based microwave radiometer data by analysing two years of measurements in central Europe. The mean overall diurnal variation was about 1.5 mm in summer and 0.5 mm in winter. Bouma (2002) analysed the diurnal variations of the IPWV using data from 30 GPS sites covering Northern Europe for a 6-year period and found that the mean amplitudes were between 0.1 and 0.6 mm

∗ Correspondence to: Surat Pramualsakdikul and Rüdiger Haas, Department of Radio and Space Science, Chalmers University of Technology, Onsala Space Observatory, SE- 439 92 Onsala, Sweden.
E-mail: surat@oso.chalmers.se; rudiger.haas@chalmers.se

in the winter months and between 0.4 and 1.6 mm in the summer months.

Most studies have concentrated on high latitude regions. The present study is focused on the area around the equator covering latitude 20 °S and 20 °N, and longitudes 70°–170 °E. The data and the analysis are presented in Section 2. Section 3 describes the procedures to obtain the diurnal and semi-diurnal amplitudes and phases. The results are presented in Section 4 and the conclusions are given in Section 5.

2. Data and analysis

GPS data available at the Scripps Orbit and Permanent Array Center (SOPAC) were used. Fourteen sites were chosen (Table I and Figure 1). All data sets were processed using the GIPSY-OASIS II software (Webb and Zumberge, 1993) with the precise point positioning (PPP) strategy (Zumberge *et al*., 1997). The GPS analysis was carried out on daily data sets plus a 3 h overlap before and after each day, resulting in 30 h long data sets. The elevation cut-off angle was set to 15° and the NMF mapping functions (Niell, 1996) were used. It is known that geophysical models can influence the estimation of atmospheric parameters from GPS (e.g. Dach and Dietrich, 2000; Vey *et al*., 2002; Watson *et al*., 2006) and that adequate ocean tide loading (OTL) models have to be used in GPS data processing. This is especially important since errors in the vertical coordinate are strongly correlated with the estimation errors of the zenith total delay (ZTD). Thus, three different GPS analyses were performed in order to study the effect of OTL on the IPWV estimates. The first analysis did not use any OTL corrections at all, and the other two used OTL corrections (Scherneck and Bos, 2002) based on two different ocean tide models, FES02 (Lefèvre *et al*., 2002) and TPXO7.0 (Egbert *et al*., 1994). Corrections for atmospheric loading were not applied. Station coordinates were estimated for all sites for each 30 h data set. The ZTD was estimated every 5 min and only the 24 h of each day were used in the following analysis.

The ZTD can be divided in to two terms – the zenith hydrostatic delay (ZHD) and the zenith wet delay (ZWD):

$$l^z = l^z_{\mathrm{h}} + l^z_{\mathrm{w}} \tag{1}$$

Table I. Site information and time span of the data acquisition.

GPS site	Site name	Geographical location		Period	Days of data
		Lat. (°)	Lon. (°)		
BAKO	Bakosurtanal	−6.48	106.85	98–04	1965
BAN2	Bangalore	13.03	77.51	03–04	705
COCO	Cocos	−12.19	96.83	98–04	2324
DARW	Darwin AU014	−12.84	131.13	98–04	1960
DGAR	Diego Garcia Islands	−7.27	72.37	98–04	1387
GUAM	USGS Guam Observatory	13.59	144.87	98–04	2199
HYDE	National Geophysical Research Institute	17.42	78.55	03–04	681
IISC	Indian Institute of Science	13.02	77.57	98–04	2052
JAB1	Jabiru AU043	−12.66	132.89	00–04	1240
KWJ1	Kwajelein Atoll	8.72	167.73	98–02	1046
LAE1	University of Technology	−6.67	146.99	01–04	1111
NTUS	Nanyang Technological University	1.34	103.68	98–04	1859
PIMO	Manila Observatory	14.64	121.08	99–04	1620
TOW2	Townsville AU028	−19.27	147.06	98–04	2294

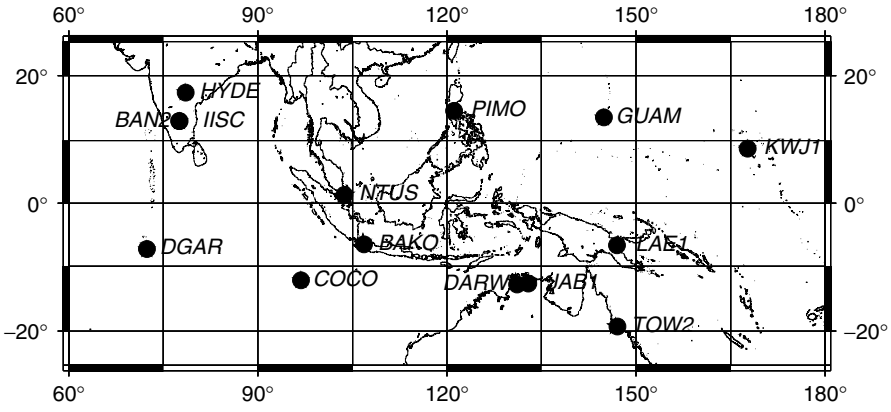

Figure 1. Map of the International GNSS Service (IGS) GPS sites used in this study.

DOI: 10.1002/met

Here l^z denotes the ZTD, l_h^z and l_w^z represent the ZHD and the ZWD, respectively. In order to infer the IPWV, first the ZHD is subtracted from the estimated ZTD. Saastamoinen (1972) presented a closed-form formula for calculating the ZHD which is dependent only on the total surface pressure and the location. Elgered *et al.* (1991) made a further development for the ZHD estimates (in mm):

$$l_h^z = (2.2779 \pm 0.0024) \times \frac{p}{f(\Phi, H)} \tag{2}$$

Here, p is the total pressure in hPa at the antenna site and

$$f(\Phi, H) = (1 - 0.00266 \times \cos 2\Phi - 0.00028 \times H) \tag{3}$$

In the above equation, Φ is the latitude and H is the height in km of the antenna above the geoid.

In the analysis, NCEP/DOE (National Centers for Environmental Prediction/Department of Energy) reanalysis-II (Kanamitsu *et al.*, 2000) ground pressure data were used to calculate the ZHD. The NCEP/DOE reanalysis-II data sets are improvements of the NCEP/NCAR (National Center for Atmospheric Research) reanalysis-I data sets (Kalnay *et al.*, 1996). These numerical weather prediction models have a temporal resolution of 6 h and a spatial resolution of $2.5^\circ \times 2.5^\circ$, and provide surface data and pressure level data at 17 levels up to a height of approximately 40 km.

The gridded pressure data were interpolated in time and space (horizontally and vertically) to the positions of the GPS sites in order to calculate the ZWD using Equations (1)–(3). Comparison of the interpolated pressure data with ground truth pressure data from radiosonde launches showed that the agreement is at the level of 0.5–1 hPa (Pramualsakdikul, 2007). An error in the total pressure of 0.5–1 hPa would cause an error of about 1–2 mm for the ZHD and approximately 0.15–0.3 mm for the IPWV.

The IPWV can be calculated from the ZWD using a conversion factor Q (Askne and Nordius, 1987):

$$Q = \frac{l_w^z}{\mathrm{IPWV}} = 10^{-8} \times (k_2' + \frac{k_3}{T_m}) \times R_w \times \rho \tag{4}$$

Here k_2' and k_3 are constants with the values of 17 ± 10 K $\times$ hPa^{-1} and 3.776×10^5 K^2 hPa^{-1}, respectively (Davis *et al.*, 1985). R_w is the specific gas constant, which is the ratio of the universal gas constant R (8.314 J mol^{-1} K^{-1}) and the molar mass of water M_w (18.0152 g mol^{-1}) and ρ is the density of liquid water (10^3 kg m^{-3}). The weighted mean temperature T_m is defined as (Bevis *et al.*, 1992):

$$T_m = \frac{\int \left(\frac{e}{T^2} \times T\right) dz}{\int \left(\frac{e}{T^2}\right) dz} \tag{5}$$

This weighting results in an approximate mean temperature of the wet refractivity in the atmosphere. In Equation (5), T is the physical temperature in K, e is the partial pressure of water vapour in hPa and z is the height.

The mean temperature T_m can be related to the surface temperature T_s. Such relations can be optimised to specific sites. Although Schüler (2001) presented results for many of the GPS sites in the present study, the linear relation presented by Bevis *et al.* (1992) has been used:

$$T_m = 70.2 + 0.72 \times T_s \tag{6}$$

Table II. IPWV mean and RMS[a] for the whole data set and the corresponding wet and dry periods.

GPS site	Whole period		Wet season			Dry season		
	Mean (mm)	RMS (mm)	Month[b]	Mean (mm)	RMS (mm)	Month[b]	Mean (mm)	RMS (mm)
BAKO	46.39	8.93	JFM	51.99	5.26	JJA	40.79	8.73
BAN2	31.90	11.66	JJA	41.68	4.38	DJF	18.48	6.31
COCO	43.32	10.68	FMA	49.07	9.84	ASO	37.46	9.28
DARW	39.03	14.89	DJF	54.67	6.87	JJA	24.26	9.36
DGAR	48.87	8.74	DJF	52.66	7.27	JJA	44.49	8.05
GUAM	45.20	10.65	JJA	51.80	6.50	JFM	36.40	9.23
HYDE	34.77	14.56	JJA	50.30	7.03	DJF	20.33	6.92
IISC	33.86	11.68	JJA	43.74	4.59	DJF	21.79	7.93
JAB1	37.10	15.09	JFM	56.07	8.77	JJA	24.18	9.06
KWJ1	47.17	10.85	JAS	53.50	5.63	JFM	37.99	10.29
LAE1	53.34	6.59	JFM	56.46	4.34	JAS	50.40	6.05
NTUS	52.62	5.42	DJF	52.41	5.55	JJA	51.26	5.23
PIMO	49.70	10.46	JAS	57.39	5.80	JFM	40.96	9.46
TOW2	33.54	13.16	DJF	45.25	11.53	JJA	22.46	8.28

[a] root-mean-square.
[b] ASO, Aug-Sep-Oct; FMA, Feb-Mar-Apr; DJF, Dec-Jan-Feb; JAS, Jul-Aug-Sep; JFM, Jan-Feb-Mar; JJA, Jun-Jul-Aug.

DOI: 10.1002/met

This was derived using data covering 2 years from 8718 radiosonde sites in the US. The impact of using Equation (6) globally has been assessed by Wang *et al.* (2005). Specifically, when studying diurnal variations the problem is that the surface temperature in general exhibits larger variability than does the mean temperature. The results presented by Wang *et al.* (2005) indicate that this error is relatively small in the area of interest. It is estimated that the error in the diurnal amplitude is less than 1% of the IPWV.

The 5 min interval ZTD values were used to calculate IPWV which then were averaged over 30 min. The resulting IPWV time series from the GPS data are shown in Figure 2.

Besides the IPWV data from the GPS analyses, IPWV data from two other sources were used, NCEP/DOE (Kanamitsu *et al.*, 2000) and ECMWF (ECMWF, 1995). These two numerical weather models (NWMs) have a temporal resolution of 6 h. Radiosonde data were not used owing to their low temporal resolution.

3. Diurnal and semi-diurnal cycle of IPWV

To study the diurnal and the semi-diurnal variability, the technique described by Dai *et al.* (2002) was followed. First, the daily mean was removed from the IPWV data sets for each day and the so-called diurnal anomalies were obtained. The wet and dry seasons, defined by the three contiguous months with the highest and the lowest precipitation, were studied separately. Table II gives the mean and root-mean-square (RMS) IPWV for the whole data sets and the corresponding wet and dry seasons. These IPWV result from GPS analysis with OTL based on the FES02 ocean tide model. The diurnal anomalies were then averaged over the three contiguous months for each season. These data were averaged over the years to obtain the mean seasonal diurnal anomalies. The mean diurnal anomalies of IPWV for each season at each GPS site were analysed with harmonic least-squares (HLS) fitting. The mean diurnal variations may be represented by (Dai *et al.*,

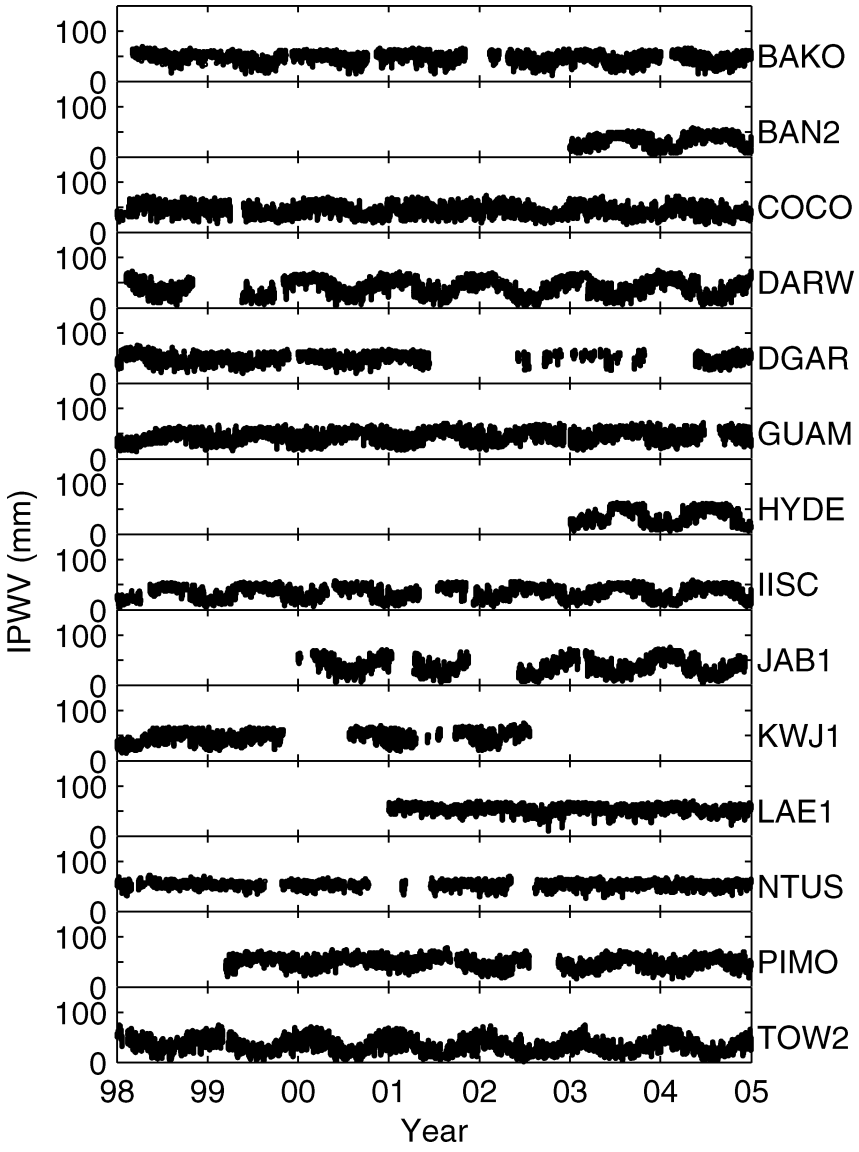

Figure 2. Time series of the IPWV at the 14 IGS sites.

DOI: 10.1002/met

2002):

$$\mathrm{IPWV}(t') = \mathrm{IPWV}_o + \sum_{n=1}^{2} S_n(t') + \varepsilon \qquad (7)$$

The summation term in the above equation is:

$$\begin{aligned} S_n(t') &= A_n \times \sin(n \times t' + \alpha_n) \\ &= a_n \times \sin(n \times t') + b_n \times \cos(n \times t') \end{aligned} \qquad (8)$$

Here, $n = 1$ and 2 denote harmonics with the periods of 24 and 12 h, respectively, IPWV_o is the daily mean value, ε is the residual, A_n is the amplitude, α_n is the phase, and t' is mean local solar time (LST) expressed in degrees or radians ($t' = 2\pi t/24$, where t is the mean LST in hours).

The Fourier transform can also be used to study the diurnal and semi-diurnal variations. However, the method requires evenly spaced data and missing data in a GPS time series are inevitable. An alternative method is then the Lomb–Scargle periodogram (LSP) (Hocke, 1998), which handles unevenly spaced data.

For validation purposes, the LSP method was used to extract the diurnal and semi-diurnal amplitude of the IPWV data for the whole data set and then the results were compared with those from the HLS fit. These IPWV data originated from the GPS data processing using OTL based on the FES02 ocean tide model.

4. Results

Figure 3 shows, as an example, the amplitude spectra from the LSP method for four IGS sites located in different environments. Strong diurnal signals are clearly seen at the BAN2 and the DARW sites located inland of a continental area, and the NTUS site which is close to the equator. The diurnal signals from these three sites are more prominent than the semi-diurnal signals. A semi-diurnal signal cannot be seen at the DARW site. However, the GUAM site, located on a small island, exhibits no clear diurnal signal but shows a weak semi-diurnal signal which may not be of atmospheric origin. Table III presents a comparison of the estimated amplitudes for all sites using both methods: the LSP and the HLS fits. For almost all sites there is agreement within 10% for both the diurnal and semi-diurnal amplitudes derived from the LSP and the HLS methods. The largest relative difference (12%) is found for the semi-diurnal signal at LAE1. The semi-diurnal signal is, in general, much smaller than the diurnal signal, except for the island sites. This fact makes a quantitative comparison more difficult. However, the diurnal signals for the sites located on the small islands such as COCO, DGAR, GUAM, and KWJ1 are weak. These four sites show semi-diurnal signals that are on the same order of magnitude as, or even larger than, the diurnal signals. Physical causes of diurnal IPWV variations are discussed in Dai *et al.* (2002). For example,

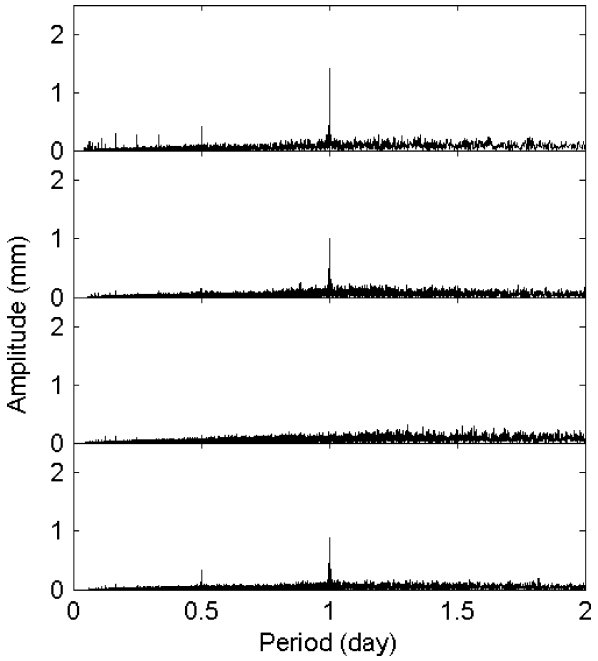

Figure 3. Amplitude spectra of GPS-derived IPWV at the four IGS sites BAN2 (top), DARW (second from the top), GUAM (third from the top) and NTUS (bottom). The spectra are based on results of 2003–2004 for BAN2 and 1998–2004 for DARW, GUAM and NTUS.

Table III. Comparison of the IPWV amplitudes derived from HLS fit and LSP method for entire period of data.

GPS site	Amplitude (mm)			
	Diurnal		Semi-diurnal	
	HLS	LSP	HLS	LSP
BAKO	2.47 ± 0.03	2.45	0.58 ± 0.03	0.60
BAN2	1.40 ± 0.02	1.40	0.40 ± 0.02	0.40
COCO	0.19 ± 0.01	0.19	0.37 ± 0.01	0.37
DARW	1.00 ± 0.02	0.99	0.12 ± 0.02	0.11
DGAR	0.23 ± 0.01	0.24	0.23 ± 0.01	0.23
GUAM	0.11 ± 0.01	0.11	0.13 ± 0.01	0.13
HYDE	0.80 ± 0.01	0.80	0.35 ± 0.01	0.35
IISC	1.27 ± 0.01	1.27	0.23 ± 0.01	0.23
JAB1	1.76 ± 0.03	1.75	0.14 ± 0.03	0.13
KWJ1	0.16 ± 0.01	0.17	0.18 ± 0.01	0.17
LAE1	1.47 ± 0.02	1.48	0.43 ± 0.02	0.48
NTUS	0.89 ± 0.01	0.89	0.29 ± 0.01	0.29
PIMO	0.66 ± 0.01	0.66	0.26 ± 0.01	0.27
TOW2	0.66 ± 0.02	0.66	0.12 ± 0.02	0.12

the observed larger amplitudes at inland sites as compared to island sites are reasonable owing to an expected larger evapotranspiration.

After the validation of the HLS fit by comparison with results from the LSP method, the analysis was concentrated specifically upen the wet and dry seasons for each site and possible differences in the IPWV variability. Identical time periods for GPS and NWM data were used. Examples of the HLS fits for three sites are shown in Figure 4. The site IISC shows large diurnal signals,

DOI: 10.1002/met

both during the wet and the dry season. The semi-diurnal signal is larger during the dry season.

The two NWMs agree better during the wet season. The site COCO shows similar IPWV variations in both seasons and it is dominated by semi-diurnal signals, while the site LAE1 reveals a large difference between the two seasons. During the wet season LAE1 has both relatively strong diurnal and semi-diurnal signals, while these are weak during the dry season.

The numerical results of the estimated diurnal and semi-diurnal signals are presented in Tables IV and V, respectively. As expected, the use of OTL corrections in the GPS data analysis does impact the IPWV amplitudes and phases. These corresponding changes are site and season dependent. There are no independent and reliable data sets with which to compare the results, but the GPS results from analyses with OTL corrections are more reasonable than the ones without OTL. It is noted that the uncertainty introduced by the use of different OTL models in the GPS data analysis does not influence the diurnal and semi-diurnal IPWV components by more than 0.08 mm in amplitude and 30 min in phase. The only exceptions are the phases of the diurnal component for DGAR, GUAM and KWJ1 with differences of up to several hours which is probably due to the small amplitudes.

The HLS fit of the GPS IPWV shows that most sites, excluding those on small islands, have significant diurnal signals with amplitudes larger than 0.4 mm, ranging up to more than 2 mm. Concerning the phases of the diurnal signals, the maxima occur typically between 1200 and 2400 local time. The four sites BAKO, DGAR, LAE1 and NTUS have large differences of the diurnal amplitudes for the wet and dry seasons. It is noted that these four sites are closest to the equator.

The agreement between the IPWV results from GPS and the two NWMs is generally poor. The NWM/GPS agreement is both site and season dependent and none of the models is consistently significantly better in agreement with GPS. However, the NWMs also give smaller diurnal amplitudes for the sites in the middle of the ocean. This may be partly explained by the amplitude error of maximum 1% introduced by the use of Equation (6). For sites with diurnal signals stronger than 1 mm the phases of NWM and GPS results typically agree within 2–4 h.

Only the IPWV data from the GPS could be used to estimate semi-diurnal components owing to the limited temporal resolution of the NWMs. The results are presented in Table IV. In general the amplitudes are smaller than 0.4 mm, with the exception of BAKO and HYDE during the dry season and LAE1 during the wet season. As for the diurnal components, it is noted that the choice of the OTL model does not influence the estimated amplitudes significantly. The use of the NCEP pressure model data, with a temporal resolution of 6 h, for the calculation of the ZHD can introduce systematic effects. The global analysis of semi-diurnal pressure variations carried out by Ray (2001) shows amplitudes between 1.0 and 1.5 hPa in this area, corresponding to 0.3–0.5 mm in IPWV. The four samples per day are marginal in order to

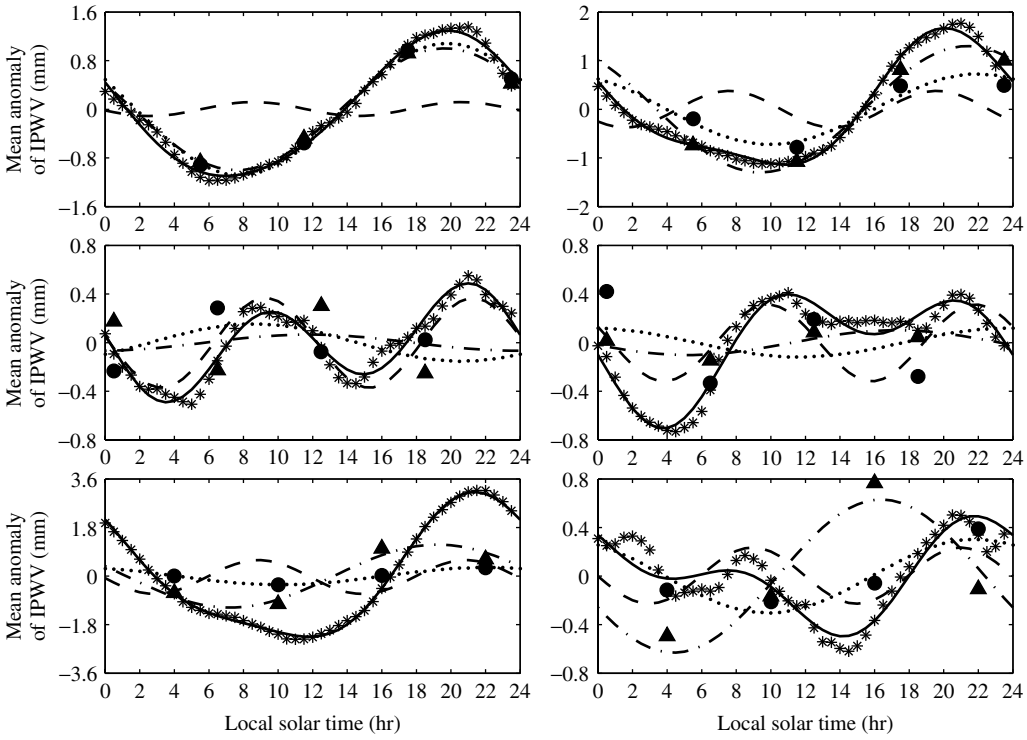

Figure 4. IPWV variability at the sites IISC (top row), COCO (middle row) and LAE1 (bottom row) during wet (left column) and dry seasons (right column). GPS, NCEP and ECMWF IPWV data are shown as crosses, circles and triangles, respectively. The black line is the two-component fit to the GPS IPWV data. The dashed line shows the semi-diurnal component only. The diurnal components of the NCEP and ECMWF IPWV data are shown as dotted and dashed-dotted lines, respectively.

DOI: 10.1002/met

Table IV. Diurnal IPWV components using no OTL, and OTL based on the TPXO7.0 and FES02 ocean tide models in the GPS processing, along with the IPWV amplitudes and phases from the NCEP and ECMWF models.

GPS site	Diurnal amplitude/phase		Method
	Wet seasony (mm/h : min)	Dry season (mm/h : min)	
BAKO	$1.38 \pm 0.03/16:35 \pm 0:05$	$3.34 \pm 0.03/19:30 \pm 0:05$	GPS, no OTL
	$1.70 \pm 0.03/16:20 \pm 0:05$	$2.96 \pm 0.05/19:50 \pm 0:05$	GPS, TPXO
	$1.70 \pm 0.03/16:15 \pm 0:05$	$2.98 \pm 0.05/19:55 \pm 0:05$	GPS, FES
	$0.04 \pm 0.10/$ [a]	$0.24 \pm 0.16/$ [a]	NCEP
	$0.91 \pm 0.32/19:25 \pm 1:20$	$1.49 \pm 0.02/20:45 \pm 0:05$	ECMWF
BAN2	$1.46 \pm 0.03/20:20 \pm 0:05$	$1.23 \pm 0.03/20:05 \pm 0:05$	GPS, no OTL
	$1.46 \pm 0.03/19:50 \pm 0:05$	$1.26 \pm 0.03/20:35 \pm 0:05$	GPS, TPXO
	$1.48 \pm 0.03/19:55 \pm 0:05$	$1.23 \pm 0.04/20:30 \pm 0:05$	GPS, FES
	$1.17 \pm 0.02/19:50 \pm 0:05$	$0.67 \pm 0.17/22:40 \pm 0:15$	NCEP
	$1.43 \pm 0.30/19:40 \pm 0:50$	$1.26 \pm 0.02/21:55 \pm 0:55$	ECMWF
COCO	$0.42 \pm 0.01/21:55 \pm 0:10$	$0.64 \pm 0.02/13:40 \pm 0:05$	GPS, no OTL
	$0.19 \pm 0.01/18:30 \pm 0:15$	$0.37 \pm 0.02/15:15 \pm 0:10$	GPS, TPXO
	$0.16 \pm 0.01/18:15 \pm 0:20$	$0.39 \pm 0.02/15:30 \pm 0:10$	GPS, FES
	$0.15 \pm 0.22/$ [a]	$0.12 \pm 0.43/$ [a]	NCEP
	$0.07 \pm 0.34/$ [a]	$0.10 \pm 0.07/$ [a]	ECMWF
DARW	$0.86 \pm 0.02/16:35 \pm 0:05$	$1.20 \pm 0.03/22:35 \pm 0:05$	GPS, no OTL
	$1.12 \pm 0.02/17:40 \pm 0:05$	$0.94 \pm 0.03/23:35 \pm 0:10$	GPS, TPXO
	$1.08 \pm 0.02/17:35 \pm 0:05$	$0.96 \pm 0.03/23:30 \pm 0:10$	GPS, FES
	$0.67 \pm 0.18/23:25 \pm 1:00$	$0.76 \pm 0.37/01:25 \pm 1:50$	NCEP
	$1.41 \pm 0.61/21:35 \pm 1:40$	$2.61 \pm 0.71/00:10 \pm 1:00$	ECMWF
DGAR	$0.46 \pm 0.03/18:15 \pm 0:15$	$0.08 \pm 0.03/09:00 \pm 1:30$	GPS, no OTL
	$0.34 \pm 0.02/18:35 \pm 0:15$	$0.05 \pm 0.03/15:45 \pm 1:55$	GPS, TPXO
	$0.32 \pm 0.02/17:40 \pm 0:15$	$0.08 \pm 0.03/20:45 \pm 1:15$	GPS, FES
	$0.24 \pm 0.21/$ [a]	$0.24 \pm 0.21/$ [a]	NCEP
	$0.38 \pm 0.11/22:15 \pm 1:05$	$0.36 \pm 0.20/03:35 \pm 2:05$	ECMWF
GUAM	$0.80 \pm 0.01/14:00 \pm 0:05$	$0.46 \pm 0.02/00:35 \pm 0:10$	GPS, no OTL
	$0.21 \pm 0.02/19:50 \pm 0:20$	$0.26 \pm 0.01/09:15 \pm 0:10$	GPS, TPXO
	$0.20 \pm 0.02/21:40 \pm 0:20$	$0.29 \pm 0.01/10:10 \pm 0:10$	GPS, FES
	$0.22 \pm 0.65/$ [a]	$0.10 \pm 0.10/$ [a]	NCEP
	$0.35 \pm 0.46/$ [a]	$0.07 \pm 0.04/18:50 \pm 2:00$	ECMWF
HYDE	$0.98 \pm 0.02/23:00 \pm 0:05$	$1.24 \pm 0.03/18:35 \pm 0:05$	GPS, no OTL
	$0.90 \pm 0.02/22:40 \pm 0:05$	$1.19 \pm 0.03/18:55 \pm 0:05$	GPS, TPXO
	$0.93 \pm 0.02/22:40 \pm 0:05$	$1.18 \pm 0.03/18:50 \pm 0:05$	GPS, FES
	$0.66 \pm 0.01/22:45 \pm 0:05$	$0.22 \pm 0.15/$ [a]	NCEP
	$0.79 \pm 0.19/22:20 \pm 0:55$	$1.10 \pm 0.01/18:55 \pm 0:05$	ECMWF
IISC	$1.17 \pm 0.02/19:45 \pm 0:05$	$1.31 \pm 0.02/19:45 \pm 0:05$	GPS, no OTL
	$1.17 \pm 0.02/19:05 \pm 0:05$	$1.34 \pm 0.02/20:20 \pm 0:05$	GPS, TPXO
	$1.19 \pm 0.02/19:10 \pm 0:05$	$1.31 \pm 0.02/20:15 \pm 0:05$	GPS, FES
	$1.08 \pm 0.04/19:25 \pm 0:10$	$0.72 \pm 0.20/21:40 \pm 1:00$	NCEP
	$1.00 \pm 0.04/19:15 \pm 0:10$	$1.30 \pm 0.05/21:05 \pm 0:10$	ECMWF
JAB1	$1.35 \pm 0.02/20:50 \pm 0:05$	$1.54 \pm 0.03/21:30 \pm 0:05$	GPS, no OTL
	$1.51 \pm 0.02/20:40 \pm 0:05$	$1.34 \pm 0.03/21:45 \pm 0:05$	GPS, TPXO
	$1.46 \pm 0.02/20:40 \pm 0:05$	$1.37 \pm 0.03/21:45 \pm 0:05$	GPS, FES
	$0.89 \pm 0.13/22:25 \pm 0:30$	$1.14 \pm 0.31/23:20 \pm 1:00$	NCEP
	$2.04 \pm 0.56/20:35 \pm 1:00$	$2.84 \pm 0.26/21:00 \pm 0:20$	ECMWF
KWJ1	$0.30 \pm 0.02/13:50 \pm 0:15$	$0.47 \pm 0.02/00:40 \pm 0:10$	GPS, no OTL
	$0.26 \pm 0.02/21:30 \pm 0:15$	$0.08 \pm 0.02/04:35 \pm 0:55$	GPS, TPXO
	$0.26 \pm 0.02/22:45 \pm 0:15$	$0.00 \pm 0.02/$ [a]	GPS, FES
	$0.45 \pm 0.76/$ [a]	$0.03 \pm 0.06/$ [a]	NCEP
	$0.99 \pm 0.57/22:25 \pm 2:10$	$0.37 \pm 0.20/23:15 \pm 2:05$	ECMWF
LAE1	$3.02 \pm 0.02/21:55 \pm 0:05$	$0.17 \pm 0.03/09:45 \pm 0:35$	GPS, no OTL
	$2.58 \pm 0.02/21:45 \pm 0:05$	$0.30 \pm 0.02/23:25 \pm 0:20$	GPS, TPXO
	$2.56 \pm 0.02/21:40 \pm 0:05$	$0.34 \pm 0.03/23:50 \pm 0:15$	GPS, FES
	$0.32 \pm 0.02/21:55 \pm 0:15$	$0.30 \pm 0.12/21:40 \pm 1:35$	NCEP
	$1.16 \pm 0.28/19:00 \pm 0:55$	$0.63 \pm 0.19/16:10 \pm 1:10$	ECMWF

(*continued overleaf*)

DOI: 10.1002/met

Table IV. (*Continued*).

GPS site	Diurnal amplitude/phase		Method
	Wet seasony (mm/h : min)	Dry season (mm/h : min)	
NTUS	$1.23 \pm 0.02/15:55 \pm 0:05$	$0.56 \pm 0.02/14:15 \pm 0:05$	GPS, no OTL
	$1.39 \pm 0.02/16:15 \pm 0:05$	$0.50 \pm 0.02/12:45 \pm 0:05$	GPS, TPXO
	$1.40 \pm 0.02/16:10 \pm 0:05$	$0.48 \pm 0.02/12:50 \pm 0:05$	GPS, FES
	$0.66 \pm 0.30/21:55 \pm 1:45$	$0.27 \pm 0.23/$ [a]	NCEP
	$0.68 \pm 0.43/23:15 \pm 2:25$	$0.74 \pm 0.42/$ [a]	ECMWF
PIMO	$1.31 \pm 0.02/17:50 \pm 0:05$	$0.44 \pm 0.01/12:45 \pm 0:10$	GPS, no OTL
	$1.00 \pm 0.02/18:40 \pm 0:05$	$0.72 \pm 0.02/13:45 \pm 0:05$	GPS, TPXO
	$1.02 \pm 0.02/18:40 \pm 0:05$	$0.72 \pm 0.02/13:40 \pm 0:05$	GPS, FES
	$0.33 \pm 0.11/17:55 \pm 1:20$	$0.16 \pm 0.13/$ [a]	NCEP
	$0.72 \pm 0.25/18:35 \pm 1:20$	$0.57 \pm 0.35/15:30 \pm 2:20$	ECMWF
TOW2	$1.00 \pm 0.02/22:45 \pm 0:05$	$0.52 \pm 0.02/17:45 \pm 0:10$	GPS, no OTL
	$0.55 \pm 0.02/21:55 \pm 0:05$	$0.72 \pm 0.02/20:25 \pm 0:05$	GPS, TPXO
	$0.53 \pm 0.02/21:30 \pm 0:05$	$0.72 \pm 0.02/20:45 \pm 0:05$	GPS, FES
	$0.56 \pm 0.09/21:15 \pm 0:40$	$0.69 \pm 0.24/23:35 \pm 1:20$	NCEP
	$1.22 \pm 0.13/22:15 \pm 0:25$	$1.20 \pm 0.27/22:30 \pm 0:50$	ECMWF

[a] Phases with formal uncertainties larger than 2.5 h are regarded as unreliable and thus not shown.

Table V. Semi-diurnal IPWV components using no OTL and OTL based on the TPXO7.0 and FES02 ocean tide models in the GPS data analysis.

GPS site	Semi-diurnal amplitude/phase		Method
	Wet season (mm/h : min)	Dry season (mm/h : min)	
BAKO	$0.06 \pm 0.03/06:00 \pm 0:15$	$0.83 \pm 0.05/07:05 \pm 0:20$	GPS, no OTL
	$0.20 \pm 0.03/08:05 \pm 0:20$	$0.92 \pm 0.05/07:15 \pm 0:20$	GPS, TPXO
	$0.18 \pm 0.03/07:55 \pm 0:20$	$0.92 \pm 0.05/07:10 \pm 0:20$	GPS, FES
BAN2	$0.42 \pm 0.03/06:20 \pm 0:20$	$0.52 \pm 0.03/06:55 \pm 0:20$	GPS, no OTL
	$0.39 \pm 0.03/06:05 \pm 0:20$	$0.49 \pm 0.03/06:45 \pm 0:20$	GPS, TPXO
	$0.39 \pm 0.03/06:05 \pm 0:20$	$0.49 \pm 0.03/06:45 \pm 0:20$	GPS, FES
COCO	$0.69 \pm 0.01/10:30 \pm 0:20$	$0.69 \pm 0.02/10:50 \pm 0:20$	GPS, no OTL
	$0.40 \pm 0.01/09:05 \pm 0:20$	$0.34 \pm 0.02/09:35 \pm 0:20$	GPS, TPXO
	$0.37 \pm 0.01/09:15 \pm 0:20$	$0.32 \pm 0.02/09:45 \pm 0:20$	GPS, FES
DARW	$0.40 \pm 0.02/12:20 \pm 0:10$	$0.14 \pm 0.03/09:50 \pm 0:20$	GPS, no OTL
	$0.33 \pm 0.02/12:25 \pm 0:10$	$0.14 \pm 0.03/08:40 \pm 0:20$	GPS, TPXO
	$0.38 \pm 0.02/12:45 \pm 0:10$	$0.06 \pm 0.03/09:10 \pm 0:20$	GPS, FES02
DGAR	$0.88 \pm 0.03/09:00 \pm 0:20$	$0.77 \pm 0.03/08:25 \pm 0:20$	GPS, no OTL
	$0.27 \pm 0.02/09:15 \pm 0:20$	$0.16 \pm 0.03/07:15 \pm 0:20$	GPS; TPXO
	$0.26 \pm 0.02/09:20 \pm 0:20$	$0.14 \pm 0.03/07:15 \pm 0:20$	GPS, FES
GUAM	$0.18 \pm 0.01/12:15 \pm 0:10$	$0.21 \pm 0.02/11:25 \pm 0:25$	GPS, no OTL
	$0.13 \pm 0.02/11:10 \pm 0:20$	$0.18 \pm 0.01/10:55 \pm 0:20$	GPS, TPXO
	$0.11 \pm 0.02/11:30 \pm 0:20$	$0.16 \pm 0.01/11:05 \pm 0:20$	GPS, FES
HYDE	$0.12 \pm 0.02/05:00 \pm 0:15$	$0.75 \pm 0.03/06:35 \pm 0:20$	GPS, no OTL
	$0.11 \pm 0.02/04:30 \pm 0:15$	$0.74 \pm 0.03/06:30 \pm 0:20$	GPS, TPXO
	$0.12 \pm 0.02/04:30 \pm 0:15$	$0.74 \pm 0.03/06:30 \pm 0:20$	GPS, FES
IISC	$0.18 \pm 0.02/08:05 \pm 0:20$	$0.41 \pm 0.02/07:15 \pm 0:20$	GPS, no OTL
	$0.12 \pm 0.02/08:20 \pm 0:20$	$0.38 \pm 0.02/07:15 \pm 0:20$	GPS, TPXO
	$0.12 \pm 0.02/08:15 \pm 0:20$	$0.38 \pm 0.02/07:15 \pm 0:20$	GPS, FES
JAB1	$0.26 \pm 0.02/12:00 \pm 0:10$	$0.22 \pm 0.03/12:00 \pm 0:20$	GPS, no OTL
	$0.22 \pm 0.02/12:10 \pm 0:10$	$0.19 \pm 0.03/12:00 \pm 0:10$	GPS, TPXO
	$0.23 \pm 0.02/12:30 \pm 0:10$	$0.19 \pm 0.03/12:20 \pm 0:10$	GPS, FES
KWJ1	$0.83 \pm 0.02/09:40 \pm 0:20$	$1.05 \pm 0.02/09:50 \pm 0:20$	GPS, no OTL
	$0.19 \pm 0.02/07:15 \pm 0:20$	$0.25 \pm 0.02/09:00 \pm 0:20$	GPS, TPXO
	$0.23 \pm 0.02/07:00 \pm 0:20$	$0.25 \pm 0.02/08:35 \pm 0:20$	GPS, FES
LAE1	$0.69 \pm 0.02/08:55 \pm 0:20$	$0.32 \pm 0.03/09:30 \pm 0:20$	GPS, no OTL
	$0.63 \pm 0.02/08:40 \pm 0:20$	$0.23 \pm 0.03/08:45 \pm 0:20$	GPS, TPXO
	$0.63 \pm 0.02/08:40 \pm 0:20$	$0.23 \pm 0.03/08:45 \pm 0:20$	GPS, FES

(*continued overleaf*)

DOI: 10.1002/met

Table V. (*Continued*).

GPS site	Semi-diurnal amplitude/phase		Method
	Wet season (mm/h : min)	Dry season (mm/h : min)	
NTUS	$0.09 \pm 0.02/11:25 \pm 0:25$	$0.37 \pm 0.02/09:15 \pm 0:20$	GPS, no OTL
	$0.03 \pm 0.02/11:30 \pm 0:20$	$0.37 \pm 0.02/08:55 \pm 0:20$	GPS, TPXO
	$0.06 \pm 0.02/10:30 \pm 0:20$	$0.41 \pm 0.02/09:00 \pm 0:20$	GPS, FES
PIMO	$0.37 \pm 0.02/11:50 \pm 0:25$	$0.42 \pm 0.01/12:15 \pm 0:10$	GPS, no OTL
	$0.25 \pm 0.02/11:15 \pm 0:20$	$0.28 \pm 0.02/12:05 \pm 0:10$	GPS, TPXO
	$0.24 \pm 0.02/11:15 \pm 0:10$	$0.27 \pm 0.02/12:10 \pm 0:20$	GPS, FES
TOW2	$0.34 \pm 0.02/11:40 \pm 0:25$	$0.14 \pm 0.02/02:05 \pm 0:15$	GPS, no OTL
	$0.29 \pm 0.02/10:35 \pm 0:20$	$0.05 \pm 0.02/06:25 \pm 0:20$	GPS, TPXO
	$0.30 \pm 0.02/10:40 \pm 0:20$	$0.04 \pm 0.02/06:30 \pm 0:20$	GPS, FES

accurately remove this effect. Since the estimated semi-diurnal signals are of the same order of magnitude, it is not appropriate to carry out a more detailed interpretation.

5. Conclusions

The variations of IPWV focusing on the diurnal and the semi-diurnal components at 14 GPS sites in southern Asia, northern Australia and in the Pacific Ocean have been studied. It is concluded that OTL models must be used in the GPS data analysis. The two different OTL models seem to be equally accurate since their use results in diurnal and semi-diurnal IPWV amplitudes that agree within 0.08 mm and phases that agree within 30 min for most of the sites. It was found that the diurnal signals were more dominant than the semi-diurnal signals for most sites, during both the wet and the dry seasons. The four sites closest to the equator show the largest seasonal differences. Sites on relatively small islands in the ocean show only weak diurnal signals. Comparisons with independent IPWV values from NWMs show in general a poor agreement, although a correlation exists between the estimated amplitudes. Furthermore, the diurnal IPWV signals from the two NWMs do not agree with each other. Their temporal resolution of 6 h does not allow derivation of the semi-diurnal components.

It appears that the continuously operating GPS sites can provide useful IPWV data with a temporal resolution of hours. Independent, accurate data for validation are needed but are difficult to acquire. The accuracy of the amplitude of the diurnal component is probably limited by the simple model (Equation (6)) used to calculate the mean temperature of the wet refractivity. An improvement can be obtained by calculation this temperature from an NWM as suggested by Wang *et al.* (2005).

Variations in the ZHD can also affect the IPWV results. In the present study the quality of pressure data limiting the accuracy of the estimated IPWV, especially for the semi-diurnal components, cannot be ruled out. Therefore, accurate and frequent pressure observations at the GPS sites are desirable. Nevertheless, it is suggested that the demonstrated method using GPS data to derive the IPWV can be used to assess the correctness of NWMs.

Acknowledgements

NCEP reanalysis-II data provided by the NOAA/OAR/ESRL PSD, Boulder, Colorado, USA, from their web site at http://www.cdc.noaa.gov/, and ECMWF operational data were used for this study. The authors would like to thank ECMWF and NCEP for providing the data. The OTL parameters were obtained from the Automatic Loading Provider (http://www.oso.chalmers.se/~loading).

References

Askne J, Nordius H. 1987. Estimation of tropospheric delay for microwaves from surface weather data. *Radio Science* **22**(3): 379–386.

Bevis M, Businger S, Herring TA, Rocken C, Anthens RA, Ware RH. 1992. GPS Meteorology: Remote sensing of atmospheric water vapor using the Global Positioning System. *Journal of Geophysical Research* **97**(D14): 15787–15801.

Bouma HR. 2002. Ground-based GPS in climate research, Lic. Thesis, Tech. Rep. L. 456, School of Electrical and Computer Engineering, Chalmers University of Technology, Sweden.

Bouma HR, Stoew B. 2001. GPS Observations of daily variations in the atmospheric water vapor content. *Physics and Chemistry of the Earth* **26**(A6–8): 389–392.

Dach R, Dietrich R. 2000. Influence of the ocean loading effect on GPS derived precipitable water vapor. *Geophysical Research Letters* **27**(18): 2953–2956.

Dai A, Wang J, Ware RH, Van Hove T. 2002. Diurnal variation in water vapor over North America and its implications for sampling errors in radiosonde humidity. *Journal of Geophysical Research* **107**(D10): 4090 DOI: 10.1029/2001JD000642.

Davis JL, Herring TA, Shapiro II, Rogers AEE, Elgered E. 1985. Geodesy by interferometry: effects of atmospheric modeling errors on estimates of baseline length. *Radio Science* **20**: 1593–1607.

ECMWF. 1995. *The Description of the ECMWF/WCRP Level III-A Global Atmospheric Data Archive*.

Egbert G, Bennett A, Foreman M. 1994. TOPEX/Poseidon tides estimated using a global inverse model. *Journal of Geophysical Research* **99**(C12): 24821–24852.

Elgered G, Davis JL, Herring TA, Shapiro II. 1991. Geodesy by radio interferometry: Water vapour radiometry for estimation of the wet delay. *Journal of Geophysical Research* **96**(B4): 6541–6555.

Güldner J, Spänkuch D. 1999. Results of year-round remotely sensed integrated water vapor by ground-based microwave radiometry. *Journal of Applied Meteorology* **38**: 981–988.

Hocke K. 1998. Phase estimation with Lomb-Scargle periodogram method. *Annales Geophysicae* **16**: 356–358.

Kalnay E, Kanamitsu M, Kistler R, Collins W, Deaven D, Gandin L, Iredell M, Saha S, White G, Woollen J, Zhu Y, Chelliah M,

Elisuzaki W, Higgins W, Janowiak J, Mo KC, Ropelewski C, Wang J, Leetmaa A, Reynolds R, Jenne R, Joseph D. 1996. The NCEP/NCAR 49-year reanalysis project. *Bulletin of the American Meteorological Society* **77**: 437–471.

Kanamitsu M, Ebisuaki W, Woolen J, Yang S, Hnilo JJ, Fiorino M, Potter GL. 2000. NCEP/DOE AMIP-II reanalysis (R-2). *Bulletin of the American Meteorological Society* **83**: 1631–1643.

Lefèvre F, Lyard FH, Le Provost C, Schrama EJO. 2002. FES99: a global tide finite element solution assimilating tide gauge and altimetric information. *Journal of Atmospheric and Oceanic Technology* **19**: 1345–1356.

Niell AE. 1996. Global mapping functions for the atmosphere delay at radio wavelengths. *Journal of Geophysical Research* **101**(B2): 3227–3246.

Pramualsakdikul S. 2007. GPS measurements of atmospheric water vapour in a low-latitude region, Thesis for the degree of Licentiate of Engineering, Technical Report No. 18L, Department of Radio and Space Science, Chalmers University of Technology, Sweden.

Ray RD. 2001. Comparisons of global analyses and station observations of the S2 barometric tide. *Journal of Atmospheric and Solar-Terrestrial Physics* **63**: 1085–1097.

Saastamoinen J. 1972. Atmospheric correction for the troposphere and stratosphere in radio ranging of satellites. In *The Use of Artificial Satellites for Geodesy*, *Geophysical Monograph Series 15*, Henriksen SW, Mancini A, Chovitz BH, (eds). AGU: Washington, DC; 247–251.

Scherneck H-G, Bos MS. 2002. Ocean tide and atmospheric loading. In *IVS 2002 General Meeting Proceedings, International VLBI Service for Geodesy and Astrometry, NASA/CP-2002-210002*, Vandenberg NR, Baver KD. NASA Goddard Space Flight Center, Greenbelt (eds); 205–214.

Schüler T. 2001. On ground-based GPS tropospheric delay estimation, PhD thesis, Universität der Bundeswehr, Munich.

Vey S, Dietrich R, Johnsen K-P, Miao J, Heygster G. 2004. Comparison of tropospheric water vapour over Antarctica derived from AMSU-B data, ground based GPS data and the NCEP/NCAR reanalysis. *Journal of the Meteorological Society of Japan* **82**(1B): 259–267.

Vey S, Calais E, Llubes M, Florsch N, Woppelmann G, Hinderer J, Amalvict M, Lalancette MF, Simon B, Duquenne F, Haase JS. 2002. GPS measurements of ocean loading and its impact on zenith tropospheric delay estimates: a case study in Brittany, France. *Journal of Geodesy* **76**: 419–427.

Wang J, Zhang L, Dai A. 2005. Global estimates of water-vapor-weighted mean temperature of the atmosphere for GPS applications. *Journal of Geophysical Research* **110**: DOI: 10.1029/2005JD006215.

Watson C, Tregoning P, Coleman R. 2006. Impact of solid Earth tide models on GPS coordinate and tropospheric time series. *Geophysical Research Letters* **33**: DOI: 10.1029/2005GL025538.

Webb FH, Zumberge JF. 1993. *An Introduction to the GIPSY/OASIS-II*. Jet Propulsion Lab. JPL Publication: Pasadena D-11088.

Zumberge JF, Heflin MB, Jefferson DC, Watkins MM, Webb FH. 1997. Precise point positioning for the efficient and robust analysis, of GPS data from large networks. *Journal of Geophysical Research* **102**(B3): 5005–5017.

DOI: 10.1002/met